THE AMERICAN SOCIETY OF MECHANICAL ENGINEERS
345 E. 47th St., New York, N.Y. 10017

95-GT-289

INFLUENCE OF LEADING-EDGE GEOMETRY ON PROFILE LOSSES IN TURBINES AT OFF-DESIGN INCIDENCE: EXPERIMENTAL RESULTS AND AN IMPROVED CORRELATION

M.W. Benner
S.A. Sjolander
Department of Mechanical and Aerospace Engineering
Carleton University
Ottawa, Ontario
CANADA

S.H. Moustapha
Pratt & Whitney Canada Inc.
Longueuil, Quebec
CANADA

ABSTRACT

The most recent correlations for turbine profile losses at off-design incidence include the leading-edge diameter as the only aspect of the leading-edge geometry which influences the losses. Cascade measurements are presented for two turbine blades which differ primarily in their leading-edge geometries. The incidence was varied over a range of ±20 degrees and the results show significant discrepancies between the observed profile losses and those predicted by the available correlations. Using data from the present experiments, as well as cases from the literature for which sufficient geometric data are given, a revised correlation has been developed. The new correlation is a function of both the leading-edge diameter and the wedge angle, and it is significantly more successful than the existing correlations. It is argued that the off-design loss behaviour of the blade is influenced by the magnitude of the discontinuity in curvature at the points where the leading-edge circle meets the rest of the blade profile. The wedge angle appears to be an approximate and convenient measure of the discontinuity in curvature at these blend points.

NOMENCLATURE

AVR = $\dfrac{\int_0^s Vx_2\, d\dot{m}}{\int_0^s Vx_1\, d\dot{m}}$ = axial velocity ratio

C = blade chord

Cp = $\dfrac{P - P_1}{\frac{1}{2}\rho V_1^2}$ = static pressure coefficient

Cp_b = $\dfrac{P_b - P_2}{\frac{1}{2}\rho V_2^2}$ = base pressure coefficient

Cx = blade axial chord

d = diameter of leading-edge circle

H = blade span

i = $\alpha_1 - \alpha_{1,\,des}$ = incidence

K = $\dfrac{v}{V^2}\dfrac{dV}{dx}$ = acceleration parameter

M = Mach number

P = static pressure

P_b = base pressure

P_0 = total pressure

s = blade pitch or spacing

t = trailing-edge thickness

V = velocity

w = $s\cos\gamma$ = passage width

We = leading-edge wedge angle (in degrees)

Y = $\dfrac{P_{0_2} - P_{0_1}}{\frac{1}{2}\rho V_2^2}$ = total pressure loss coefficient

α = flow angle, measured from the axial direction

β = blade metal angle, measured from the axial direction

γ = blade stagger angle, specific heat ratio

δ = boundary layer thickness

δ^* = $\int_0^\delta \left(1 - \dfrac{V}{V_e}\right) dy$ = boundary layer displacement thickness

θ = $\int_0^\delta \dfrac{V}{V_e}\left(1 - \dfrac{V}{V_e}\right) dy$ = boundary layer momentum thickness

Presented at the International Gas Turbine and Aeroengine Congress & Exposition
Houston, Texas - June 5-8, 1995
This paper has been accepted for publication in the Transactions of the ASME
Discussion of it will be accepted at ASME Headquarters until September 30, 1995

ρ = fluid density

υ = fluid viscosity

ϕ^2 = $\dfrac{V_2^2}{V_{2,is}^2}$ = kinetic energy coefficient

= $\dfrac{\textit{actual outlet kinetic energy}}{\textit{kinetic energy for isentropic expansion}}$

χ = $\left(\dfrac{d}{s}\right)^{-0.05} We^{-0.2} \left(\dfrac{\cos\beta_1}{\cos\beta_2}\right)^{-1.4} \left[\alpha_1 - \alpha_{1,des}\right]$

= new incidence parameter (angles in degrees)

χ' = $\left(\dfrac{d}{s}\right)^{-1.6} \left(\dfrac{\cos\beta_1}{\cos\beta_2}\right)^{-2} \left[\alpha_1 - \alpha_{1,des}\right]$

= Moustapha et al. incidence parameter (α_1 measured in degrees)

Subscripts

des = value at the design point

e = boundary-layer edge value

P = profile value

x = axial direction

1,2 = cascade inlet and outlet, respectively

INTRODUCTION

Turbine design is an iterative process involving a trade-off between the aerodynamic performance at design and off-design conditions. Furthermore, the design will be influenced by non-aerodynamic factors. For example, durability considerations will impose certain cross-sectional area and maximum thickness requirements on the airfoils. These requirements might be met by using large leading-edge diameters. However, large leading-edge diameters will increase the losses and heat loads at the design condition, due to the increase in size of the associated horseshoe vortices. On the other hand, the large diameters will make the airfoils more tolerant to off-design incidence. Thus, a careful balance must be struck in the design process in an effort to satisfy a large number of sometimes conflicting requirements.

Empirical loss correlations and meanline analysis continue to play an important role in this process, particularly in the early stages of design. Therefore, there is an on-going need to review and improve these correlations.

Probably the most widely used empirical loss system for axial turbines is that due to Ainley & Mathieson (1951). The Ainley & Mathieson system is a complete system in that it includes correlations for all the components of the loss and for both design and off-design conditions. It was subsequently modified by Dunham & Came (1970) to reflect the improved understanding of some aspects of the flow, notably the secondary flows. Further improvements to the design-point correlations were presented by Kacker & Okapuu (1981). Craig & Cox (1971) and a few other researchers have also proposed complete loss systems, but these are not as widely used as those based on Ainley & Mathieson's work.

In 1990, Moustapha et al. (1990) reviewed the available correlations for profile and secondary losses at off-design conditions and compared them with a range of recent measurements. The authors concluded that the existing correlations do not adequately account for recent improvements in airfoil design and are no longer as reliable as they once were. Based on the substantial database of measurements which they had collected, the authors devised new correlations for the profile and secondary losses. These were significantly more successful at correlating the data than the Ainley & Mathieson correlations. Drawing on the work of Mukhtarov & Krichakin (1969), and unlike Ainley & Mathieson, Moustapha et al. included the leading-edge diameter as a correlating parameter. The new off-design correlations were intended for use with the Kacker & Okapuu design-point correlations to form a complete loss system.

To verify the Moustapha et al. correlations and to investigate further the influence of the leading-edge geometry on the off-design behaviour of turbine blades, an experimental study was initiated in a low-speed cascade wind tunnel. This paper presents the results obtained for the profile losses. Two blade designs which differ mainly in their leading-edge geometries have been investigated. Based on the results an improved correlation for off-design profile losses is introduced.

EXPERIMENTAL RESULTS

Cascade Test Section

All measurements presented here were obtained in the linear cascade test section shown schematically in Figure 1. Two cascades, designated CC2 and CC3, were examined. The sets of five blades are mounted on a turntable which allows the incidence to be varied over a wide range. The side flaps and tailboards are used to adjust the inlet flow uniformity and the outlet flow periodicity.

The data for CC2 were obtained primarily during a study of the effects of axial velocity ratio (AVR) on turbine cascade measurements (Rodger et al., 1992). The endplates shown in the figure are adjustable and allow the divergence of the streamtube through the cascade, and thus the axial velocity ratio, to be varied. For both cascades in the present study, the AVR was varied at each incidence to provide data over a range which included AVR = 1.0. The loss coefficients presented here are the interpolated values at AVR = 1.0. In addition to adjusting the AVR values, the spanwise distributions of the losses were examined at all values of incidence. In all cases there was a reasonable extent of constant loss about the midspan of the blade. Thus, the results are as two-dimensional as can be reasonably achieved in a cascade of fairly low aspect ratio.

All measurements were made at a constant Reynolds number of $3.0 \pm 0.1 \times 10^5$ based on inlet velocity and true chord. The velocity at the cascade inlet was typically about 30 m/s so that conditions were essentially incompressible. The normal turbulence intensity at the cascade inlet is about 0.3% and most measurements were

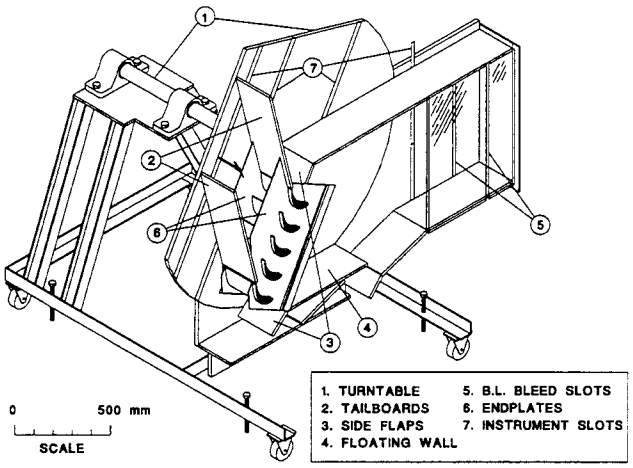

Fig. 1. Schematic of Variable-Incidence Test Section.

obtained under these conditions. The inlet turbulence intensity for CC3 was also increased to about 3% using a grid (Whitehouse, et al., 1993), but this was found to have very little effect on the loss behaviour of this blade: at both design and off-design incidence, differences in measured losses were close to the uncertainty in the measurements.

Blade and Cascade Geometries

The geometries of the two cascades are summarized in Figure 2. Cascade CC2 represents the midspan section of a power turbine blade. This cascade has been used extensively in the past primarily for studies of off-design profile losses (eg. Goobie et al., (1989), Tremblay et al., (1990), and Rodger et al. (1992)). After the development of the Moustapha et al. (1990) correlation, cascade CC3 was fabricated to examine further the influence of leading-edge geometry on the off-design losses. The two blades were designed for same inlet and outlet flow conditions using the same turbine-profile design system.

As shown on Figure 2, CC3 has a leading-edge diameter roughly twice that of CC2. This would normally be expected to reduce the sensitivity to off-design incidence. To maintain similar blade pressure distributions for the two blades, which required that maximum thickness be essentially the same and at the same chordwise location, the leading-edge wedge angle for CC3 was reduced to 43° from the value of 52.4° used for CC2. Figure 3 shows that the pressure distributions measured for the two blades at the design incidence were in fact very similar.

Experimental Procedures

All flowfield measurements were obtained with a three-hole pressure probe. The probe tip had a width of 2 mm and a thickness of 0.7 mm. The probe pressures were measured with capacitive-type pressure transducers and recorded using a microcomputer-based data acquisition system. The corresponding flow quantities are estimated to have the following accuracies: total and dynamic pressures, ±1% of the local dynamic pressure;

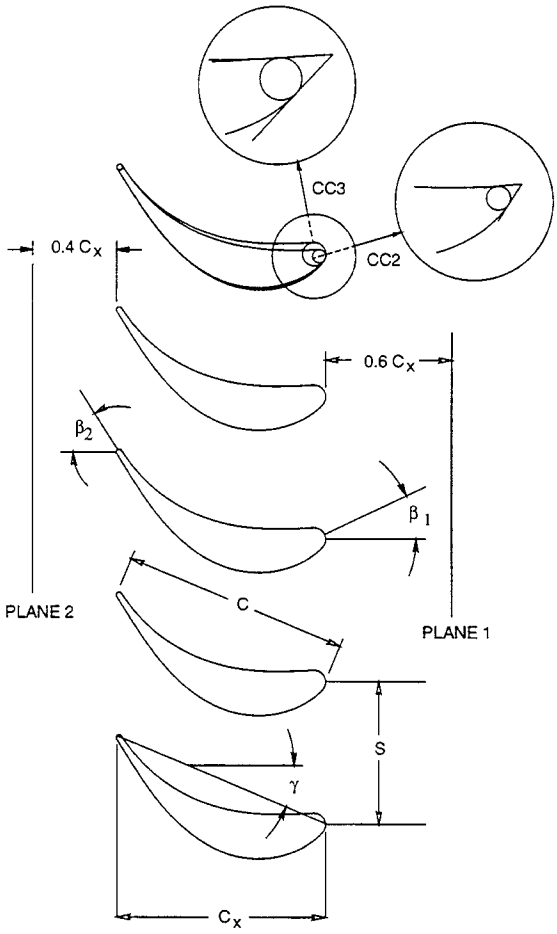

Cascade Parameters		
	CC3	CC2
Blade span, H (mm)	200	200
Blade spacing, S (mm)	110.7	110.7
True chord, C (mm)	162.3	162.8
Axial chord, Cx (mm)	149.4	150.0
Stagger angle, γ (deg.)	21.6	23.1
t_{MAX}/C	0.196	0.182
Inlet metal angle, β_1 (deg.)	25.5	29.3
Outlet metal angle, β_2 (deg.)	57.5	57.5
Leading-edge diameter (mm)	16.7	9.43
Leading-edge wedge angle (deg.)	43.0	52.4
Trailing-edge thickness (mm)	4.2	4.2

Fig. 2. Blade and Cascade Geometries.

flow angles, ±0.5°; and mass-averaged total-pressure loss coefficients, ±5%. The values of incidence angle are estimated to be accurate to ±0.5°.

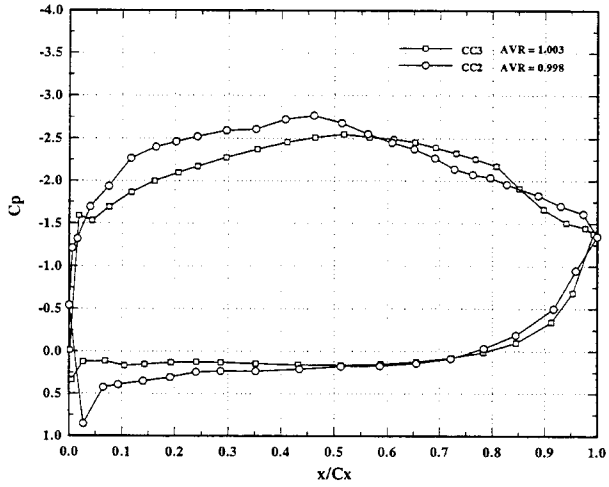

Fig. 3. Blade Pressure Distributions at Design Incidence.

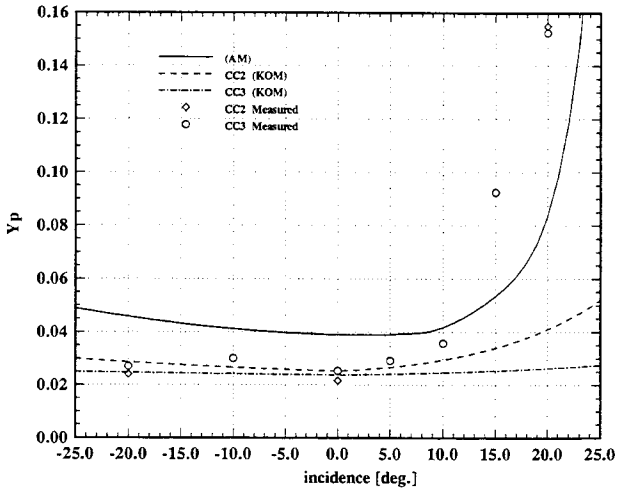

Fig. 4. Variation of Midspan Loss Coefficients.

One blade from each cascade is also instrumented with 11 rows of static taps, each row having 43 taps. One of the taps is located on the trailing edge to give the base pressure. For the present measurements only the midspan rows of taps were used.

The locations of the upstream and downstream traverse planes are indicated on Figure 2. The losses quoted later are fully mixed-out values calculated assuming mixing at constant area from the downstream plane.

Results for Off-Design Incidence

Figure 4 shows the measured profile loss coefficients for the two cascades as a function of incidence. The corresponding predictions using the classical Ainley & Mathieson (AM) and the Kacker & Okapuu/Moustapha et al. (KOM) loss systems are also shown. The AM values are essentially the same for the two blades since the only relevant parameter which varied was the maximum thickness-to-chord ratio and it changed by only a small amount. While the KOM system matches the data somewhat better, the change in losses predicted by the Moustapha et al. correlation, due to the change in leading-edge diameter, was not reflected in the data for CC2 and CC3 at positive incidence. This suggests a need to re-examine the influence of leading-edge geometry on off-design profile losses.

It should be mentioned that data for CC2 had earlier been compared with the Moustapha et al. correlation with apparently better agreement than is shown here, notably at large positive incidence (Tremblay et al., 1990). However, these earlier measurements were conducted at rather large values of axial velocity ratio (estimated at as high as 1.08 for +20 degrees of incidence). Concern about the effect of this on the measurements led to the investigation of AVR by Rodger et al. (1992). This study showed that modest flow convergence (AVR > 1.0) has only a mild effect on the measured losses, provided there is no significant trailing-edge separation. However, when separation is present the imposed favourable pressure gradient which is implied by AVR > 1.0 has the effect of shifting the separation point closer to the trailing edge. At a given incidence, this leads to lower profile losses than would be the case for more closely two-dimensional flow. As a result, the Tremblay et al. measurements gave lower losses at large positive incidence and therefore better agreement with the correlation..

For use in later discussion, some of the blade pressure measurements are also presented.

Figure 5 shows the variation in the blade pressure distributions at positive incidence for CC3. As incidence increases, a velocity overshoot appears on the suction side at the leading edge and, whereas at design incidence the flow is accelerated up to about midchord, at higher values of incidence the flow is decelerated along the full length of the suction surface. Figure 6 shows the pressure distributions for the two blades at +20 degrees of incidence. The mismatch in static pressures at the trailing edge is probably the result of the difference in the axial velocity ratios for the two sets of measurements. However, the difference in the suction peaks on the forward part of the blades seems to be too large to explain in this way. Nor does the uncertainty in the incidence angle seem adequate to explain the difference. In fact, the suction peak would have been expected to be milder for CC3 because of its larger leading-edge diameter. Instead, some other factor is evidently amplifying the suction peak.

As already noted, the agreement between the present measurements and the Moustapha et al. correlation was somewhat poor. This prompted a re-examination of the correlation and the results of this are presented next.

IMPROVED CORRELATION

Discussion

As will be shown later, the Moustapha et al. correlation for off-design profile losses has been modified to include the effect of the leading-edge wedge angle. This resulted in a noticeable

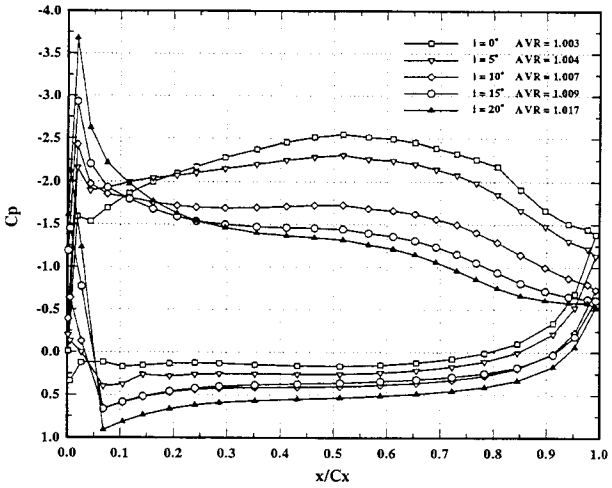

Fig. 5. Effect of Positive Incidence on Blade Pressure Distributions (CC3).

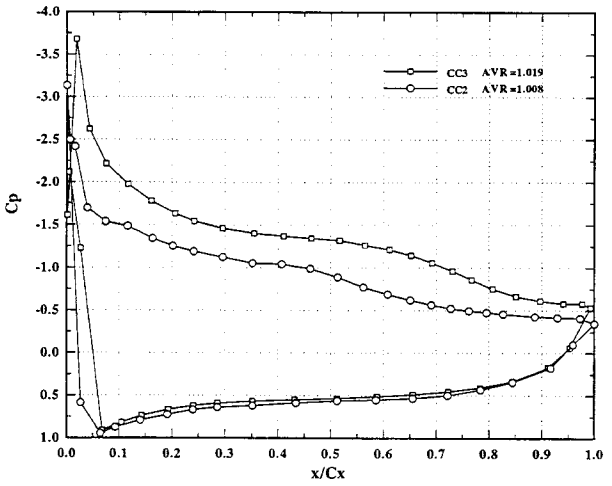

Fig. 6. Blade Pressure Distributions at +20^{O} Incidence.

improvement in agreement with the present experimental data as well as with the data from the literature for which the wedge angle was available. This section examines the physical relationship between the leading-edge geometry and the profile losses, in an attempt to explain why the wedge angle should appear in the correlation.

The importance of the details of the leading-edge geometry has been recognized for some time. For example, Stow (1985) discusses the redesign of the leading edge of a turbine airfoil to remove a "spike", or local overshoot, in velocity very close to the leading edge. Stow does not explicitly identify the origin of the spike, but it appears to be associated with the blend point where the leading-edge circle meets the rest of the suction-side profile. It is plausible that a pressure disturbance would occur at this point since there would normally be a discontinuity in curvature there.

In his detailed examination of the boundary layer on a turbine rotor blade, Hodson (1985) likewise noted the occurrence of a sharp velocity overshoot at the blend point. As Hodson observed, this overshoot may often be missed in blade loading measurements since it is of short extent and can easily fall between static taps. This is almost certainly the case for the present measurements with CC2 and CC3. Hodson found that the bubbles quickly reattached since the velocity overshoot occurred in a region of overall favourable pressure gradient. In fact, he concluded that transition was not necessarily completed in the bubbles and that the subsequent favourable pressure gradient could in any case cause relaminarization of the boundary layer.

More recently, Walraevens & Cumpsty (1993) specifically examined the leading-edge flow using a plate mounted in a wind tunnel. The incidence and the freestream turbulence were varied and both circular and elliptic leading edges were considered. Separation occurred at the same point, a short distance upstream of the blend point, under most conditions. The authors explicitly link the likelihood of separation to the magnitude of the discontinuity in curvature at the blend point. Thus, the appearance of separation was delayed to a higher angle of incidence for the elliptic leading edge because of its milder discontinuity in curvature. Raising the level of freestream turbulence shortened the separation bubble somewhat but, for the circular leading edge in particular, did not prevent the appearance of the separation bubble or change the location of the separation. Boundary-layer measurements made downstream of the bubbles showed a substantial increase in momentum thickness as the extent of the bubble increased. This loss of momentum would be due to the mixing losses occurring in the free shear layer as well as the fact that the layer reattached turbulent. It should be noted that for all of the cases considered, the bubbles were reattaching in a region of adverse pressure gradient.

The profile losses are taken to include the loss production in the blade-surface boundary layers as well as at the trailing edge. With some simplifying assumptions, Denton (1993) relates the profile losses to the boundary layer parameters at the trailing edge and the trailing edge conditions as follows:

$$Y = \frac{2\theta}{w} + \left(\frac{\delta^* + t}{w}\right)^2 - \frac{C_{P_b} t}{w} \qquad (1)$$

where t is the trailing-edge thickness and w is the passage width. The first term accounts for the direct loss production in the boundary layers. The momentum thickness in this term is particularly influenced by the location of boundary-layer transition as well as by the mixing at the edge of any separation bubbles which may be present. The second term is the sudden-expansion loss at the trailing edge, where the blockage associated with the boundary-layer displacement thickness contributes to the effective change in area. The final term accounts for the retarding force which would be exerted by a low base pressure. The influence of the leading-edge geometry on the profiles losses should thus be

explained mainly through its influence on the boundary-layer parameters at the trailing edge. This influence would be expected to make itself felt mainly up to the onset of trailing-edge separation, at which point the last two terms begin to dominate the losses. The boundary layers on the suction surface of turbomachinery blades are normally turbulent by the time they reach the trailing edge. Thus, although the onset of separation is influenced by the thickness of the incoming boundary layer, the angle of incidence at which separation begins should be determined mainly by the blade pressure distribution. Therefore, any conclusions about the influence of the leading-edge geometry on losses are expected to hold mainly for negative incidence and for positive incidence up to the onset of significant trailing-edge separation.

In the light of Equation (1) and the earlier experimental studies, the following picture is proposed for CC2 and CC3.

Considering first the design incidence, both profiles experience a leading-edge velocity spike, although in the measured results (Figure 3) this was evident only for CC3. Figure 7 shows the suction-surface velocity distributions for both profiles as predicted using a blade-to-blade potential flow code. It is clear that the spikes are directly related to the two blend points. The blend point for CC3 is further from the leading edge, consistent with the smaller wedge angle. As noted earlier, the wedge angle was chosen to give roughly the same maximum thickness for the two profiles. However, on geometric grounds the smaller wedge angle will also tend to give a larger discontinuity in curvature at the blend point, and this is confirmed by the stronger velocity spike experienced by CC3. The strong adverse pressure gradient immediately after the spike may be sufficient to separate the boundary layer which will be laminar at that point. Normally transition would occur quickly in a laminar separation bubble, which then allows it to reattach. However, since the overall pressure gradient quickly reverts to strongly favourable, a transitional or even laminar separation bubble should be able to reattach here. Furthermore, even if transition had commenced it might well be followed by relaminarization due to the acceleration. The value of the acceleration parameter K is in fact higher than the suggested critical value (eg. Mayle, 1991) of about 3×10^{-6} for a short length after the velocity spike. In any event, surface flow visualization conducted on the suction surface of both blades strongly suggested that transition occurred naturally over a distance from about 50 to 70% of the chord length. Thus, while separation bubbles might have been present, they were evidently very short and did not trigger transition. For both reasons, they would have had relatively little effect on the boundary-layer development and therefore on the losses generated on the blade surfaces.

The picture changes as the incidence becomes positive. As seen from Figure 5, at positive incidence a normal overspeed develops at the leading edge. At the higher values of incidence a short separation bubble was also apparent from the surface flow visualization. Furthermore, once the incidence exceeds about 10 degrees the pressure gradient is adverse over essentially the whole of the suction surface. As a result of the adverse pressure gradient, the leading-edge separation will begin to have a greater

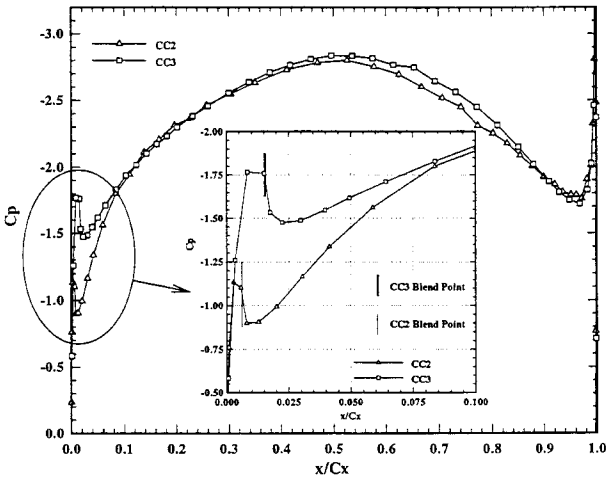

Fig. 7. Predicted Flow around Leading Edge at Design Incidence (Potential Flow Calculation).

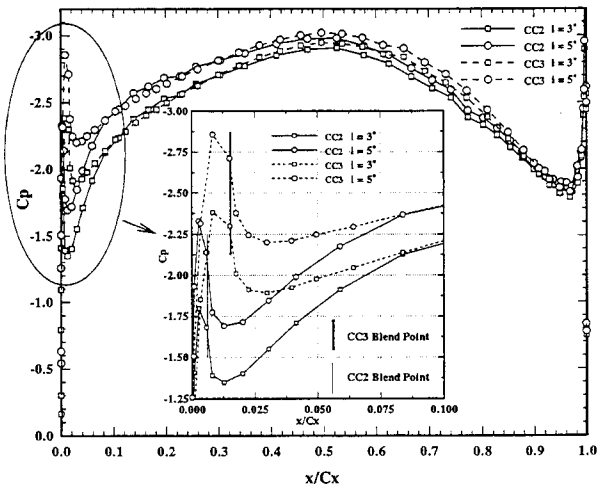

Fig. 8. Predicted Flow around Leading Edge - Effect of Incidence (Potential Flow Prediction).

influence on the losses: the bubble will tend to be longer, with greater loss production, and transition will probably be necessary for its reattachment. In turn, a geometric factor which tends to make the bubble larger will also tend to increase the losses. Potential-flow calculations for the flow in the leading-edge region of both blades are shown in Figure 8 for a small range of positive incidence angles. It is seen that at a given incidence the velocity spike continues to be stronger for CC3 than for CC2, whereas one would have expected the larger diameter of CC3 to moderate the overshoot. The blade-surface measurements also showed consistently higher suction peaks for CC3, as indicated in Figure 5. Thus, it appears that the curvature discontinuity continues to influence the flow by amplifying the normal suction peak at the

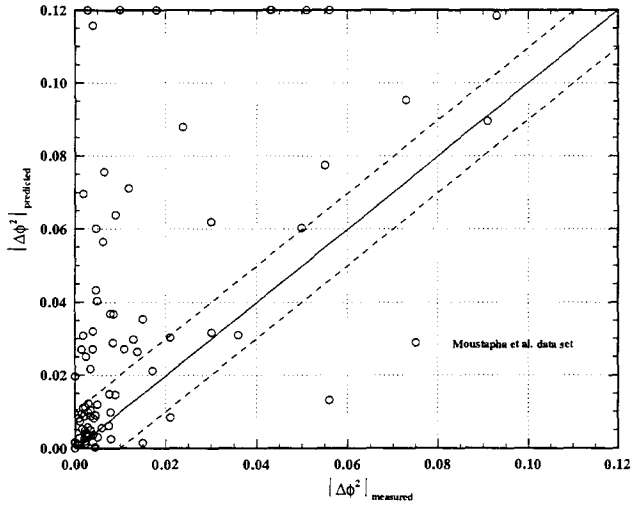

Fig. 9. Evaluation of Ainley & Mathieson Profile Loss Correlation (Predicted vs Measured).

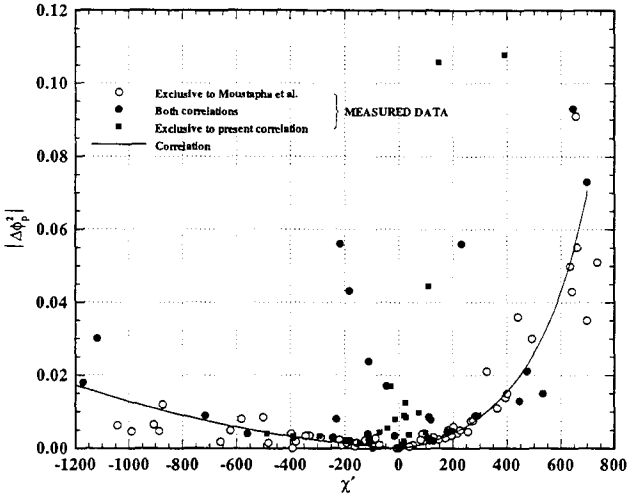

Fig. 10. Moustapha et al. (1990) Correlation for Profile Losses at Off-Design Incidence.

leading edge. For these reasons, one would likewise expect the curvature discontinuity to continue to influence the profile losses, at least up to the appearance of significant separation at the trailing edge.

For negative incidence, the discontinuity in curvature at the pressure-side blend point comes into play to encourage the occurrence of a pressure-side separation bubble. This bubble is expected to reattach under most circumstances, but the mixing at the edge of this and the likely turbulent state of the subsequent boundary layer will increase the loss production on the pressure surface. Again, these losses will be influenced by the severity of the discontinuity in curvature through its influence on the appearance and chordwise extent of the separation bubble.

To summarize, it is believed, as has been suggested by a few other researchers, that the strength of the discontinuity in curvature at the leading-edge blend points will influence the trend in losses at off-design values of incidence. Obviously, it would be very inconvenient to have the curvature discontinuity appear explicitly in the profile-loss correlation. However, it is suggested that the value of the leading-edge wedge angle is a reasonable, approximate measure of the curvature discontinuity: larger values of wedge angle will tend to produce smaller discontinuities, and vice versa. Therefore, the use of the wedge angle in the revised correlation is interpreted as a convenient alternative to using the curvature discontinuity directly.

New Correlation

The new correlation is a revised version of the correlation of Moustapha et al. (1990). The latter correlation was based on data from 19 cascades. Unfortunately, the values of the leading-edge wedge angles were not quoted for all of these cascades. Therefore, the present correlation is based on a subset of 8 of the cascades from the earlier database together with data for CC2, CC3 and the three cascades of Perdichizzi & Dossena (1993), for

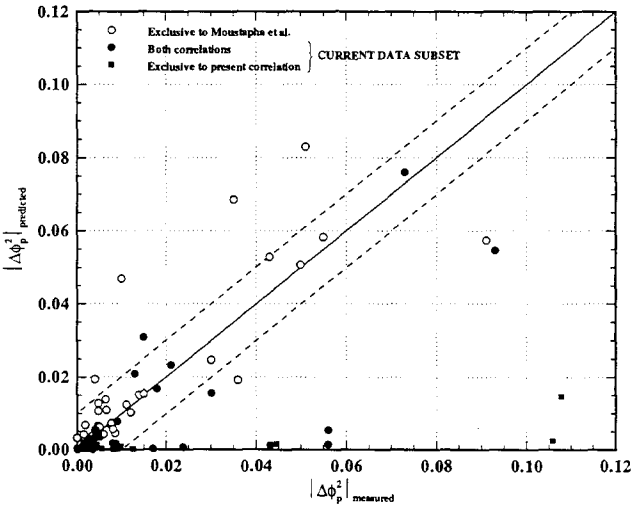

Fig. 11. Evaluation of Moustapha et al. Correlation.

a total of 13 cascades. Data for a very wide range of wedge angles and ratios of leading-edge diameter-to-spacing are included. Those sources of data which are in the open literature are identified in the list of references.

To demonstrate the improvements achieved with successive correlations, the data are compared with the Ainley & Mathieson, the Moustapha et al., and, finally, the new correlation.

Figure 9 compares the incremental losses predicted by the Ainley & Mathieson correlation with the measured values, expressed as changes to the kinetic-energy coefficient. Predicted values of $|\Delta\phi^2|$ which exceeded 0.12 have been plotted along the top edge of the figure. Ainley & Mathieson's correlation was based on cascade data obtained in the 1940's and 50's whereas the

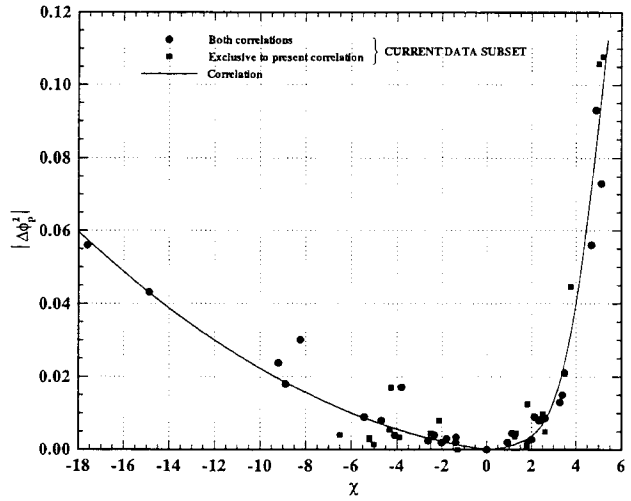

Fig. 12. Improved Correlation for Profile Losses at Off-Design Incidence.

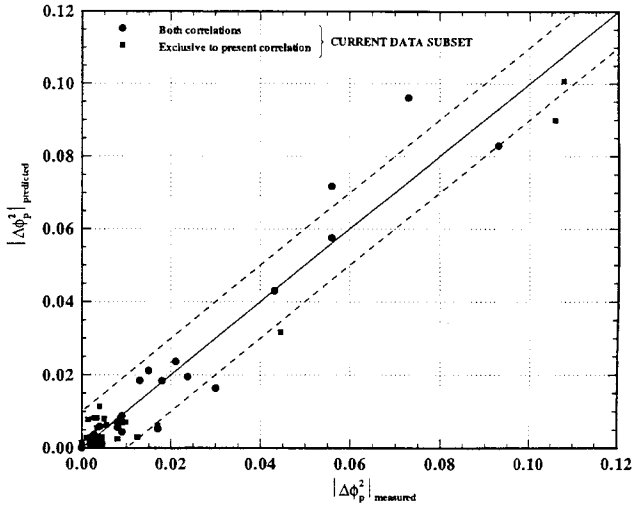

Fig. 13. Evaluation of Improved Correlation.

measured values are mostly from cascades of recent design. As might be expected, the Ainley & Mathieson correlation does not reflect the improvements in turbine design and tends to over predict the off-design losses.

Moustapha et al. correlated the incremental losses with the incidence, the channel acceleration and the ratio of the leading-edge diameter to the spacing using the incidence parameter

$$\chi' = \left(\frac{d}{s}\right)^{-1.6}\left(\frac{\cos\beta_1}{\cos\beta_2}\right)^{-2}\left[\alpha_1 - \alpha_{1,des}\right].$$

The resulting correlation is shown in Figure 10 and the evaluation of its accuracy is shown in Figure 11. Comparison with Figure 9 shows that it is significantly more successful than the Ainley & Mathieson correlation, although it still noticeably over or under predicts the losses for some cascades.

The new correlation is shown in Figure 12 and the corresponding evaluation in Figure 13. The new incidence parameter takes the form

$$\chi = \left(\frac{d}{s}\right)^{-0.05} We^{-0.2}\left(\frac{\cos\beta_1}{\cos\beta_2}\right)^{-1.4}\left[\alpha_1 - \alpha_{1,des}\right].$$

As indicated, the influence of the leading-edge diameter is now much smaller and a significant dependence on wedge angle has been introduced. The revised correlation is seen to be considerably more successful in correlating the data. This applies equally to cascades CC2 and CC3, the data for which are included on the figures. Even the data at large positive incidence seem to be quite well correlated. However, the rapid rate of increase in the losses makes the collapse of the data appear slightly better than it actually is. This is evident from Figure 13 where the largest differences between predictions and measurements are seen to occur at large values of incidence (that is, for large values of $|\Delta\phi^2|$) Nevertheless, the correlation must be regarded as excellent. For use in computations, the following polynomials have been fitted to the data:

$$\Delta\phi_P^2 = a_8\chi^8 + a_7\chi^7 + a_6\chi^6 + a_5\chi^5 + a_4\chi^4 + a_3\chi^3 + a_2\chi^2 + a_1\chi \qquad (2a)$$

where

$a_8 = +3.711\times10^{-7}$, $a_7 = -5.318\times10^{-6}$, $a_6 = +1.106\times10^{-5}$,
$a_5 = +9.017\times10^{-5}$, $a_4 = -1.542\times10^{-4}$, $a_3 = -2.506\times10^{-4}$,
$a_2 = +1.327\times10^{-3}$, $a_1 = -6.149\times10^{-5}$,

for $\chi \geq 0$, and

$$\Delta\phi_P^2 = 1.358\times10^{-4}\chi^2 - 8.720\times10^{-4}\chi \qquad (2b)$$

for $\chi < 0$.

Like the Moustapha et al. correlation, the new one is expressed in terms of a change to the kinetic-energy coefficient, ϕ^2, because that parameter varies more weakly with Mach number than does, for example, the more usual total-pressure loss coefficient, Y. However, conversions between ϕ^2 and Y are easily made using

$$Y = \frac{\left[1 - \frac{\gamma-1}{2}M_2^2\left(\frac{1}{\phi^2} - 1\right)\right]^{-\frac{\gamma}{\gamma-1}} - 1}{1 - \left(1 + \frac{\gamma-1}{2}M_2^2\right)^{-\frac{\gamma}{\gamma-1}}} \qquad (3)$$

where M_2 is the Mach number at the outlet of the blade row.

CONCLUSIONS

Measurements have been made of the off-design profile losses for two turbine blades which differ primarily in their leading-edge geometries. The recent correlation of Moustapha et al. predicted that the blade with the larger leading-edge diameter would be considerably less sensitive to incidence. However, the losses were very similar for the two blades over a wide range of incidence angles. This prompted a re-examination of the influence of the leading-edge geometry on profile losses. It was found that a significantly better correlation could be obtained by including the leading-edge wedge angle as an additional and more influential correlating parameter. It is believed that the off-design behaviour of the blade is influenced by the magnitude of the discontinuity in curvature at the blend points where the leading-edge circle joins the rest of the profile. The value of the wedge angle appears to give an approximate and convenient indication of the magnitude of this discontinuity in curvature.

The present results were obtained exclusively from blades employing leading-edge circles. It would appear that an elliptic leading edge allows a blade to be designed with milder curvature jumps at the blend points. This probably explains the reduced sensitivity to incidence which is usually attributed to elliptic leading edges.

Finally, although the present work has focussed exclusively on the influence of the leading-edge geometry on the off-design profile losses, it is recognized that there are additional factors which should be investigated. These include the Reynolds number, the turbulence intensity and the chordwise pressure distribution. The influence of the outlet Mach number is especially important and is still not well understood. It is planned to investigate some of these factors in future studies.

ACKNOWLEDGMENTS

Financial support for this study provided by the Natural Sciences and Engineering Research Council of Canada and by Pratt & Whitney Canada Inc. is gratefully acknowledged.

REFERENCES

Ainley, D.G., and Mathieson, G.C.R., 1951, "A Method of Performance Estimation for Axial Flow Turbines," ARC R&M 2974.

Aronov, B.M., Bogatyrev, A.G., Epifanov, V.M., Mamaev, B.I., and Shkurikhin, I.B., 1975, "Experimental Study of Blade Inlet Angle Influence on Profile Cascade Effectiveness," Soviet Aeronautics, Vol. 18, No.3, pp. 82-86. [Data]

Craig, H.R.M., and Cox, H.J.A., 1971, "Performance Estimate of Axial Flow Turbines," Proceedings, Institution of Mechanical Engineers, Vol. 185, No. 32, pp. 407-424.

Denton, J.D., 1993, "Loss Mechanisms in Turbomachines," ASME Trans., J. Turbomachinery, Vol. 115, pp. 621-656.

Dunham, J., and Came, P.M., 1970, "Improvements to the Ainley/Mathieson Method of Turbine Performance Prediction," ASME Trans., J. Eng. for Power, Vol. 92, pp. 252-256.

Goobie, S.M., Moustapha, S.H., and Sjolander, S.A., 1989, "An Experimental Investigation of the Effect of Incidence on the Two-Dimensional Performance of an Axial Turbine Cascade, " Proceedings, Ninth International Symposium on Air Breathing Engines, Vol. 1, pp. 197-204.

Hodson, H.P., 1985, "Boundary-Layer Transition and Separation Near the Leading Edge of a High-Speed Turbine Blade," ASME Trans., J. Eng. for Gas Turbines and Power, Vol 107, pp. 127-134.

Hodson, H.P., and Dominy, R.G., 1987a, "The Off-Design Performance of a Low-Pressure Turbine Cascade," ASME Trans., J. Turbomachinery, Vol. 109, pp. 201-209. [Data]

Hodson, H.P., and Dominy, R.G., 1987b, "Three-Dimensional Flow in a Low-Pressure Turbine Cascade," ASME Trans., J. Turbomachinery, Vol. 109, pp. 177-185. [Data]

Kacker, S.C., and Okapuu, U., 1982, "A Mean-Line Prediction Method for Axial Flow Turbine Efficiency," ASME Trans., J. Eng. for power, Vol. 104, pp. 111-119.

Mayle, R.E., 1991, "The Role of Laminar-Turbulent Transition in Gas Turbine Engines," ASME Trans., J. Turbomachinery, Vol. 113, pp. 509-537.

Moustapha, S.H., Kacker, S.C., and Tremblay, B., 1990, "An Improved Incidence Losses Prediction Method for Turbine Airfoils," ASME Trans., J. Turbomachinery, Vol. 112, pp. 267-276.

Mukhtarov, M.K., and Krichakin, V.I., 1969, "Procedure of Estimating Flow Section Losses in Axial Flow Turbines when Calculating their Characteristics," Teploenergetika, 16 (7), pp. 76-79.

Perdichizzi, A. and Dossena, V., 1993, "Incidence Angle and Pitch-Chord Effects on Secondary Flows Downstream of a Turbine Cascade," ASME Trans., J. Turbomachinery, Vol. 115, pp. 383-391. [Data]

Rodger, P., Sjolander, S.A., and Moustapha, S.H., 1992, "Establishing Two-Dimensional Flow in a Large-Scale Planar Turbine Cascade," AIAA Paper 92-3066. [Data]

Stow, P., 1985, "Incorporation of Viscous-Inviscid Interactions in Turbomachinery Design," in "Thermodynamics and Fluid Mechanics of Turbomachinery", A.S. Ucer, P. Stow, and. Ch. Hirsch eds., Nijhoff, Dordrecht, Vol. 2, pp. 887-921.

Tremblay, B., Sjolander, S.A., and Moustapha, S.H., 1990, "Off-Design Performance of a Linear Cascade of Turbine Blades," ASME Paper 90-GT-314. [Data]

Vijayaraghavan, S.B., and Kavanagh, P., 1988, "Effect of Free-Stream Turbulence, Reynolds Number, and Incidence on Axial Turbine Cascade Performance," ASME Paper 88-GT-152. [Data]

Walraevens, R.E., Cumpsty, N.A., 1993, "Leading Edge Separation Bubbles on Turbomachinery Blades," ASME Paper 93-GT-91, to be published.

Whitehouse, D.R., Moustapha, S.H., and Sjolander, S.A., 1993, "The Effect of Axial Velocity Ratio, Turbulence Intensity, Incidence, and Leading Edge Geometry on the Midspan Performance of a Turbine Cascade," Canadian Aeronautics and Space Journal, Vol. 39, No. 3, pp. 150-156. [Data]

Yamamoto, A., and Nouse, H., 1988, "Effects of Incidence on Three-Dimensional Flows in a Linear Turbine Cascade," ASME Trans., J. Turbomachinery, Vol. 110, pp. 486-496. [Data]